FIXED PATTERN NOISE IN IUE SPECTRA

Ralph C. Bohlin
ST ScI
November 1987

I. INTRODUCTION

Co-addition of n IUE spectra does not improve the signal-to-noise ratio (S/N) by the square root of n, as expected for independent random noise. Instead, a residual fixed pattern noise (FPN) dominates the noise after addition of more than $\sim$ 4 spectra. The source of this FPN is probably in the intensity transfer function (ITF) that is used to photometrically correct IUE images. Each of the 11–12 intensity levels in the ITF for the SWP and LWR cameras is an average of four flat field images from a mercury pen-ray lamp, where the dominant emission is in the 2537 Å line. The ITF for the LWP camera is still the original "mini-ITF" made from only one image per level and is poor for science that requires good S/N.

A large fraction of the signal in an unwidened spectrum is in the central pixel, even though the slit length used for the extraction is 12.7 pixels in low dispersion. Thus, the noise in the ITF for that central pixel will produce a fixed error (FPN) for that pixel for all spectra that are exposed to the same level. Historically, all attempts to reduce the FPN in the ITF by smoothing of the images at each ITF level have resulted in rather poorly documented failures. As pointed out by C. Imhoff at the IUE S/N Workshop, smoothing by properly fitting analytic functions to the data number (DN) for each pixel as a function of ITF intensity should greatly reduce FPN, if the FPN is due to noise in the ITF. However, the British are rumored to have thoroughly investigated this possibility before launch with no success. Because of the promise of greatly improved S/N in principle, the past work on fitting the individual ITFs should be reviewed.

If each pixel in an IUE image is an independent photometer as suggested by the failure of spatial smoothing techniques, then the limitation due to the motions of fixed features with respect to the line and sample readout grid should be kept in mind. This thermal instability of the analog circuitry in the readout electronics requires a resampling of the images and places a fundamental limit on the precision of any photometric correction. The SWP camera exhibits shifts in reseau positions as large as 1.5 pixels, while the LWR is stable to typically < 0.3 pixel (Thompson, Turnrose, and Bohlin 1982). Any misalignment, especially systematic misalignment, of the spectral images with the ITF can cause FPN, *even if the misalignment is a fraction of a pixel.*

The purpose of this paper is to quantitatively document the existence of FPN, using properly exposed, low dispersion spectra of BD+28°4211. A stab at the question of "how fixed is the FPN" is taken for underexposed spectra of BD+28°4211 and for properly exposed spectra of BD+75°325.

II. EVIDENCE FOR FPN IN CO-ADDED SPECTRA

Regions of the low dispersion spectrum of BD+28°4211 with no evidence for spectral lines in either high or low dispersion are chosen for measurement of S/N. Groups of 1–16 spectra are co-added, a quadratic least square fit is made, the summed spectra are divided by the fit, and the residuals about unity are measured as noise. Figures 1–4 show these results for the selected wavelength regions. Persistent patterns emerge from the random noise when many spectra are added together, as can be seen most clearly in the comparison between the summations for 4 and 8 independent spectra. As a further confirmation of the existence of FPN, Figures 5–8 show summations for two separate groups of 16 spectra for BD+28°4211 and one group of 16 for BD+75°325, as well as a summation of high dispersion spectra of BD+28°4211 that has been smoothed to low dispersion resolution. The high dispersion spectrum demonstrates that spectral features do not contribute significantly to the FPN in low dispersion, except for one line at 1720 Å in BD+75°325. All low dispersion spectra are extracted from their images with the sampling interval of 0.7 pixel and corrected for the loss in sensitivity with time in 5 Å bins according to Bohlin and Grillmair (1988a) for SWP and Bohlin and Grillmair (1988b) for LWR. The S/N is defined on a sample-to-sample basis with no smoothing or binning. Any intercomparison with other work must be on the same basis. The SWP spectra were all co-added on the sampling intervals from the production processing, which begins at 1000 Å and has a wavelength scale that agrees to better than 1 Å among all co-added spectra. The LWR spectra were all resampled to a common grid beginning at 1800 Å with an interval of 1.8693 Å.

Figures 9–10 summarize the S/N results for well exposed SWP and LWR spectra, respectively, as a function of the square root of the mean signal level in linearized flux number (FN) units. Since a photon-limited S/N is proportional to the square root of the signal, the theoretical S/N is a straight line, which can be estimated from the total FN of the co-added spectra along with the conversion to DN and the mean number of quantum events per DN from Bohlin *et al.* 1980. In general, the curves flatten out at a limiting S/N of 35–50 for SWP and 20–30 for LWR. In other words, the noise is mostly FPN for a summation of 8 spectra. A doubling of the signal to 16 spectra just doubles the noise, so that the S/N asymptotically approaches a constant for each region at high FN.

III. WHY IS THERE FPN?

If the FPN is caused by noise in the ITF, then the limiting S/N should be lower for weak exposures, and the pattern should not correlate with the pattern at higher exposure levels. In an attempt to check this behavior, exposures at the 0.3–0.7 level are co-added and displayed at the top of Figures 5–8. Unfortunately, only 3 SWP and 7 LWR point source spectra for BD+28°4211 are available, making the SWP result inconclusive. For LWR, there is a suggestion of some correlation of the pattern with the results for the 1.0 exposure level. If the FPN at the two levels do correlate, then the FPN cannot be due to noise in the ITF.

Three additional possibilities for the dominant cause of the FPN are: 1) A systematic misalignment of the data images with the ITF, which could be caused by a software bug or by differential effects of the charge distribution on the readout beam between spectral and flat field images. 2) The ITF is obtained with 2537 Å light and is not the appropriate flat field for other wavelengths. Unfortunately, BD+28°4211 has too much spectral structure to check for the disappearance of FPN near 2537 Å. 3) There is a slow secular change in the cameras.

A proper comparison of the FPN in co-added spectra between the 50 and 100% exposure levels can distinguish the possibilities suggested for the main source of the pattern. No correlation in the pattern would favor noise in the ITF, while a similar pattern at all levels would suggest that 1) or 2) above is the correct answer. A similar pattern with worse limiting S/N at low signal would favor 1), while case 2) should have comparable limiting S/N at low and high exposure levels. Note that 16 spectra at a 50% exposure have the same co-added signal as 8 spectra at 100%. Perhaps, additional observations at the 50% level are required. Possibility 3) would be easy to test using the new ITF2 obtained in the 1984 time frame. Co-added spectra obtained in the same 1984 epoch and processed with ITF2 should show less FPN than for other years, if 3) is correct. A comparable strength but a different pattern in the FPN for ITF2 would point strongly to noise in the ITFs as the prime source of the FPN. Clearly, more analysis of this problem is needed.

If noise in the ITF is a significant contributor to the FPN, then more flat field data should be obtained to improve the S/N of the ITFs.

REFERENCES

Bohlin, R. C., and Grillmair, C. J. 1988a, *Ap. J. Suppl.*, Feb. 15.

ibid 1988b, in preparation.

Bohlin, R. C., Holm, A. V., Savage, B. D., Snijders, M. A. J., and Sparks, W. M. 1980, *Astr. Ap.*, **85**, 1.

Thompson, R. W., Turnrose, B. E., and Bohlin, R. C. 1982, *Astr. Ap.*, **107**, 11.

FIGURE CAPTIONS

Fig. 1–2. S/N in low dispersion spectra of BD+28°4211 in selected wavelength regions. From the top, the number of spectra summed for each plot is 1, 1, 2, 4, 8, and 16. The corresponding SWP numbers used for each plot are 14426; 17944; 14671 and 14783; 18067, 15324, 18446, and 18881; 16004, 16712, 16960, 17087, 17180, 17373, 17578, and 17693; and the sum of all 16 listed above for the bottom plot.

Fig. 3–4. Same as Figures 1–2 for the LWR camera. The LWR numbers for the top 5 plots are 11834; 15077; 12210 and 12321; 12976, 13243, 13371, and 15968; 13623, 13854, 14165, 14166, 14542, 14887, 14935, and 15071.

Fig. 5–6. S/N in SWP spectra of BD+28°4211 for 4 cases in each wavelength region, plus one case for BD+75°325. From the top, the cases are the sum of 3 weak exposures in the 30–70% exposure range, the same 16 exposures at the 100% level shown in Fig. 1–2, another group of 16 exposures at the 100% level, 16 exposures at 100% for BD+75°325, and the sum of 4 high dispersion spectra smoothed to low dispersion resolution.

Fig. 7–8. S/N in long wavelength spectra for 6 cases in each wavelength region. All spectra are of BD+28°4211, except the 4th from the top. All spectra are LWR, except the bottom one. From the top, the cases are the sum of 7 weak exposures in the 30–70% range, the same 16 exposures at the 100% level shown in Fig. 3–4, another group of 16 exposures at the 100% level, 16 exposures at 100% for BD+75°325, the sum of 7 LWR high dispersion spectra smoothed to low dispersion resolution, and the sum of 4 LWP high dispersion spectra smoothed to low dispersion resolution.

Fig. 9–10. S/N as a function of the square root of the signal in IUE FN units for the co-added low dispersion spectra of BD+28°4211. The straight line is the theoretical quantum noise limit to the S/N.

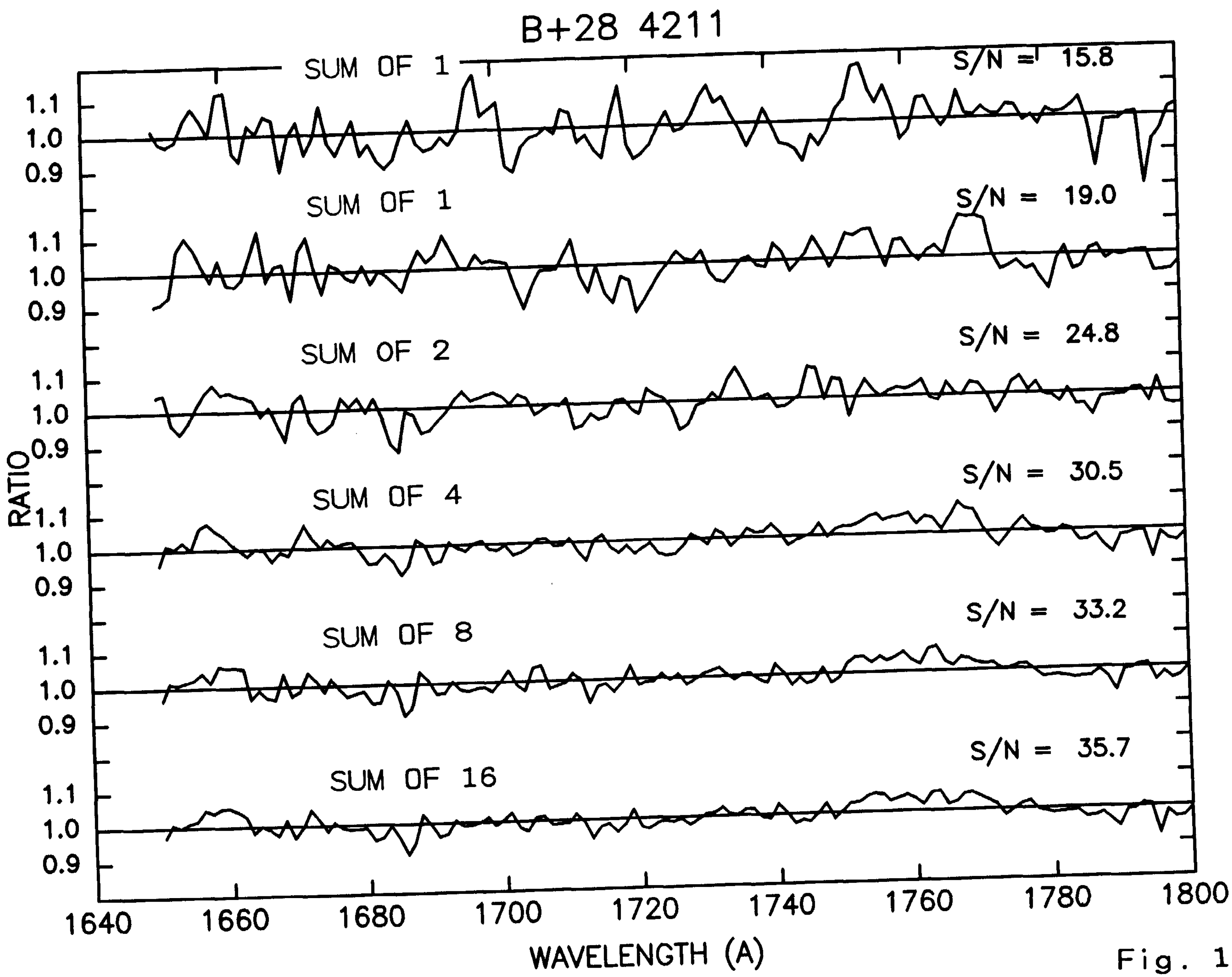

B+28 4211
SUM OF 1
S/N = 15.8
SUM OF 1
S/N = 19.0
SUM OF 2
S/N = 24.8
SUM OF 4
S/N = 30.5
SUM OF 8
S/N = 33.2
SUM OF 16
S/N = 35.7
RATIO
1.1
1.0
0.9
1640
1660
1680
1700
1720
1740
1760
1780
1800
WAVELENGTH (A)

Fig. 1

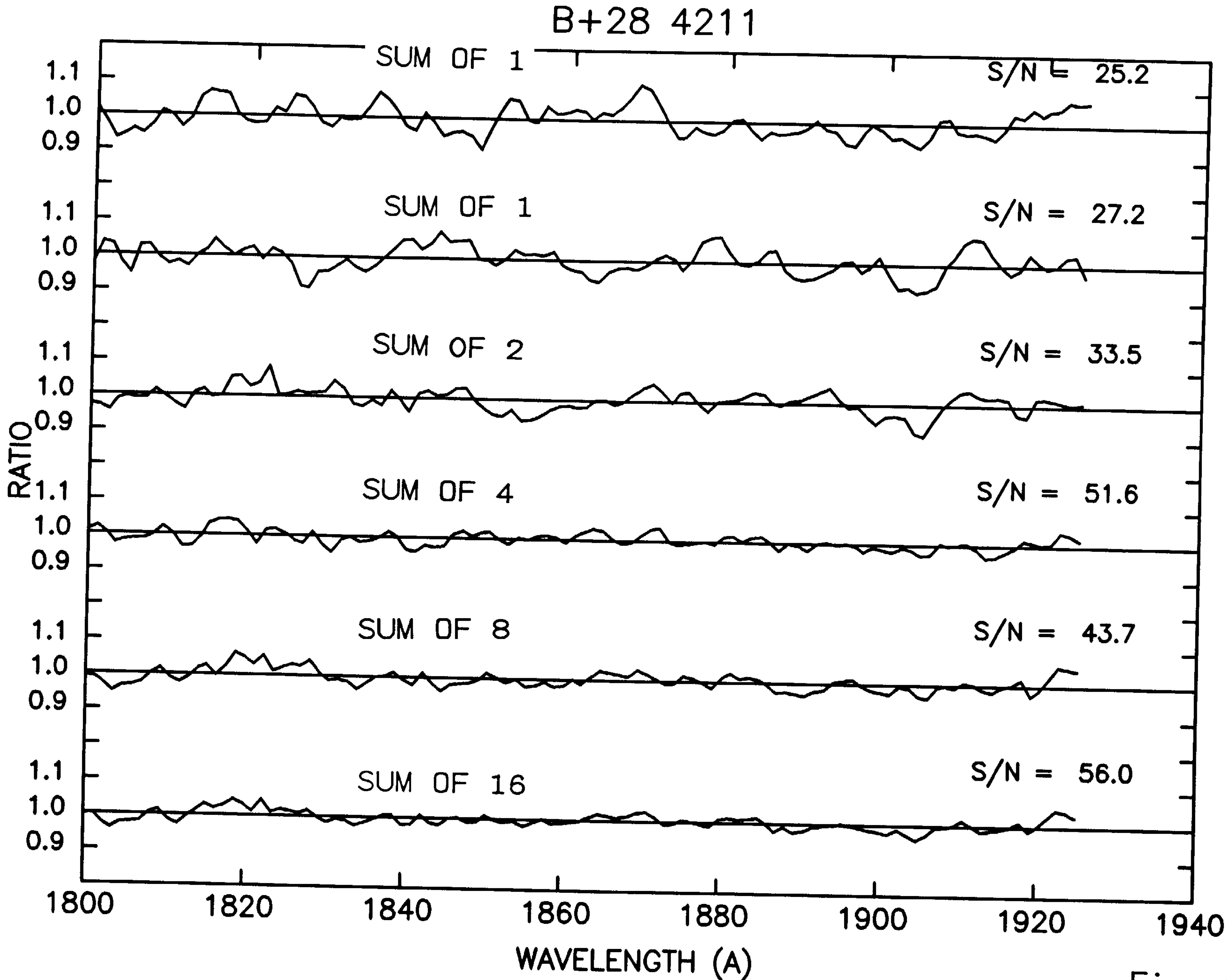
B+28 4211
SUM OF 1
S/N = 25.2
SUM OF 1
S/N = 27.2
SUM OF 2
S/N = 33.5
SUM OF 4
S/N = 51.6
SUM OF 8
S/N = 43.7
SUM OF 16
S/N = 56.0
RATIO
1.1
1.0
0.9
1800
1820
1840
1860
1880
1900
1920
1940
WAVELENGTH (A)

Fig. 2

16

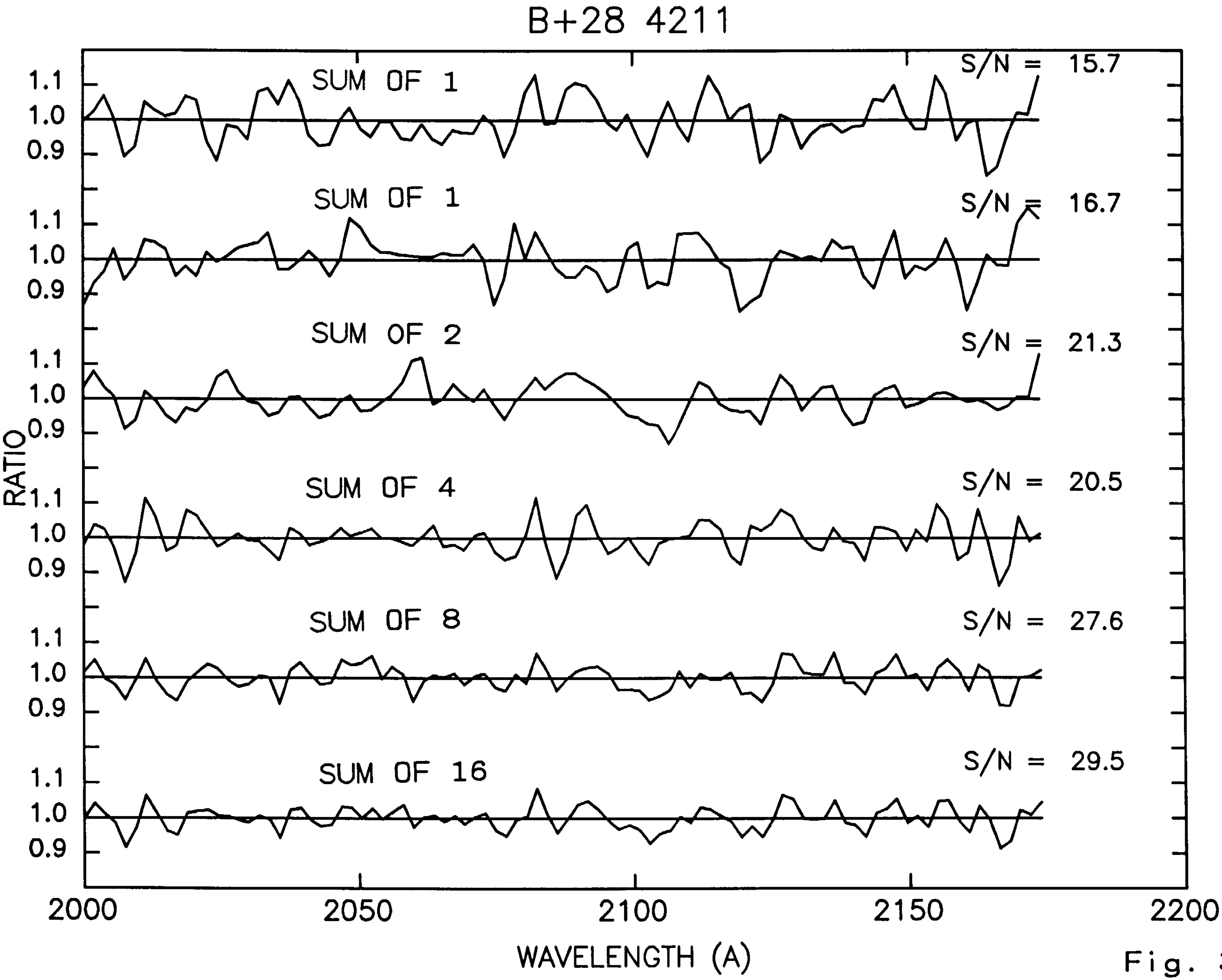

B+28 4211
SUM OF 1
S/N = 15.7
SUM OF 1
S/N = 16.7
SUM OF 2
S/N = 21.3
SUM OF 4
S/N = 20.5
SUM OF 8
S/N = 27.6
SUM OF 16
S/N = 29.5
1.1
1.0
0.9
RATIO
2000
2050
2100
2150
2200
WAVELENGTH (A)

Fig. 3

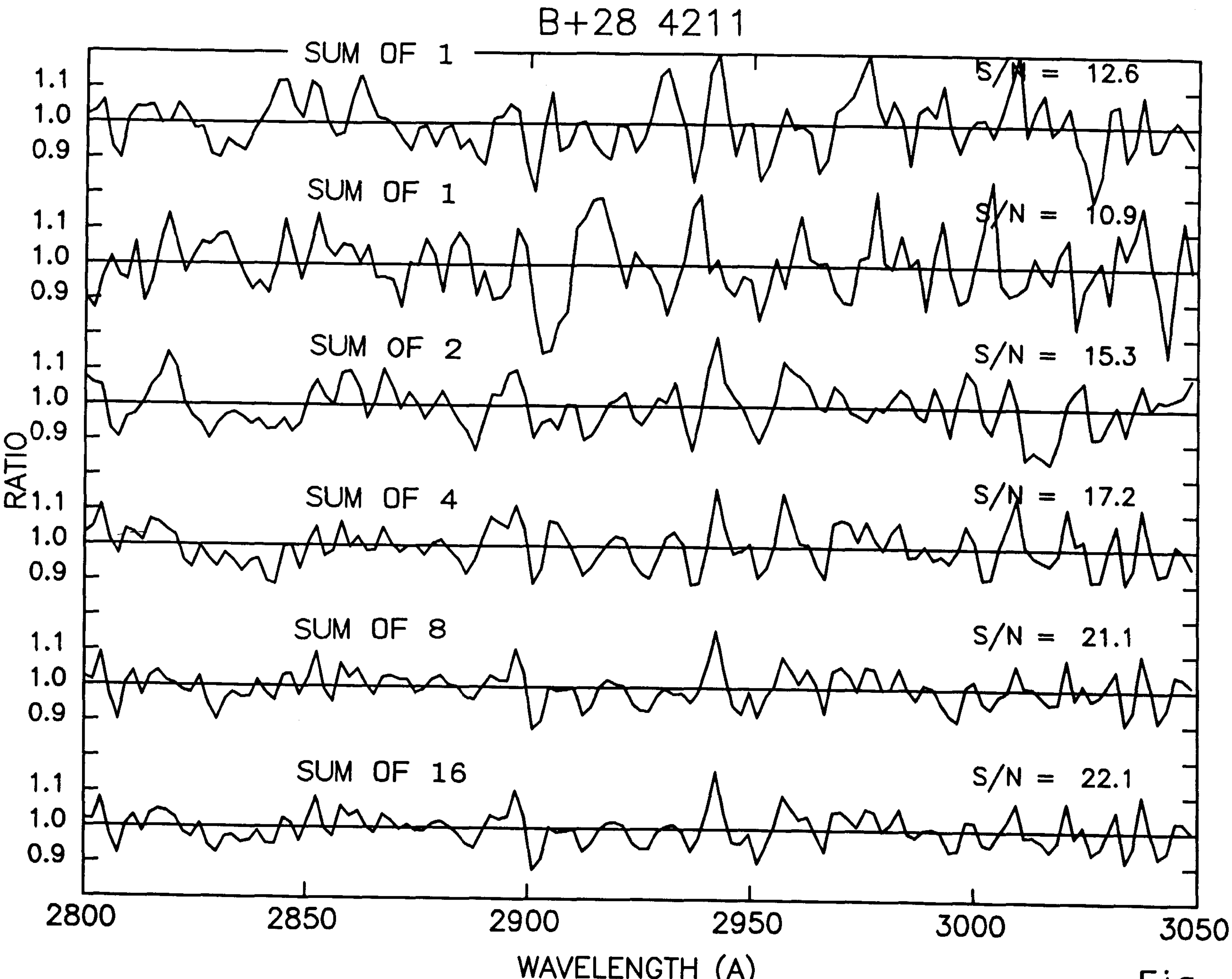

B+28 4211
SUM OF 1
S/N = 12.6
SUM OF 1
S/N = 10.9
SUM OF 2
S/N = 15.3
SUM OF 4
S/N = 17.2
SUM OF 8
S/N = 21.1
SUM OF 16
S/N = 22.1
1.1
1.0
0.9
RATIO
2800
2850
2900
2950
3000
3050
WAVELENGTH (A)

Fig. 4

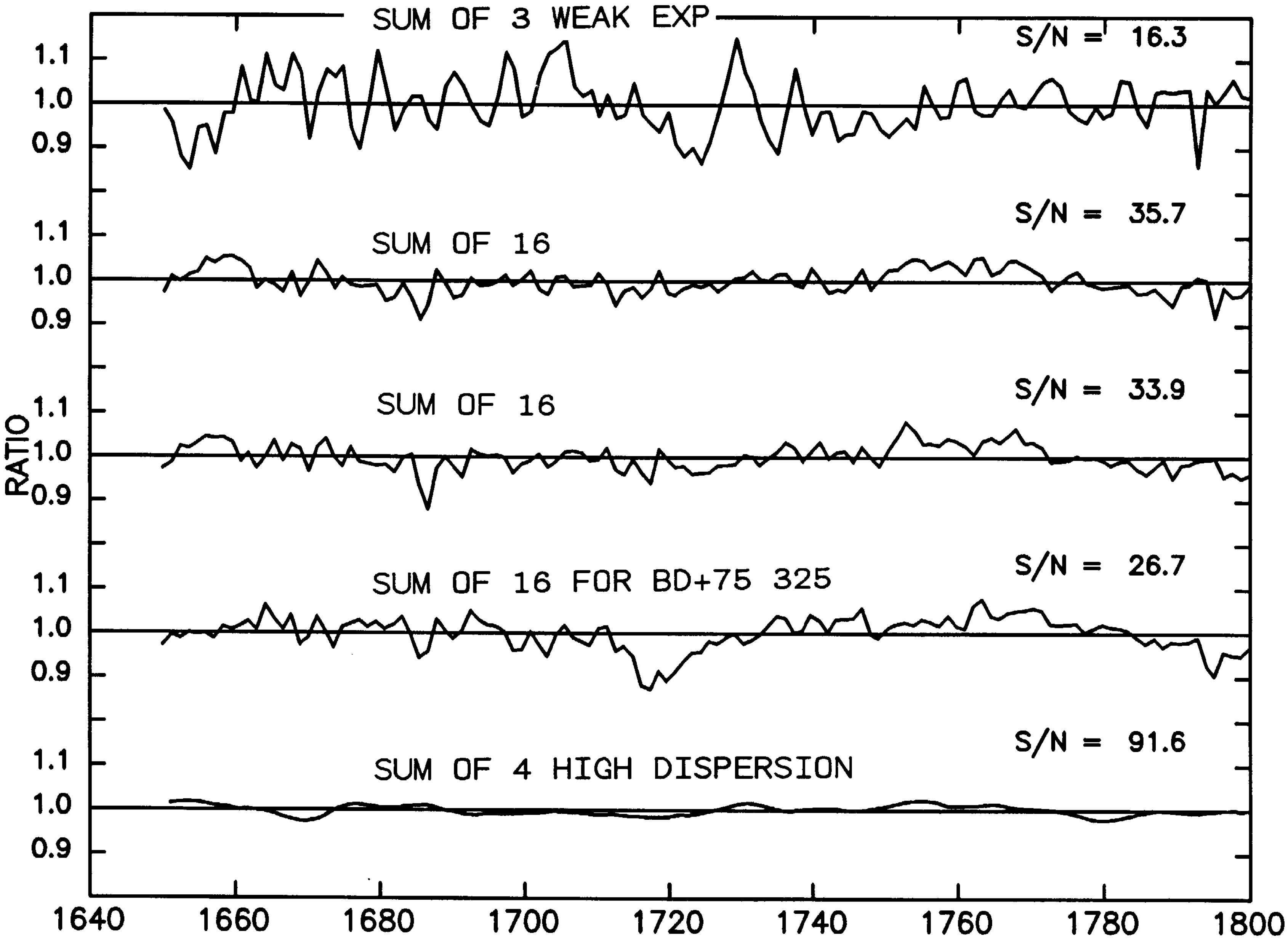

SUM OF 3 WEAK EXP
S/N = 16.3
SUM OF 16
S/N = 35.7
SUM OF 16
S/N = 33.9
SUM OF 16 FOR BD+75 325
S/N = 26.7
SUM OF 4 HIGH DISPERSION
S/N = 91.6
1.1
1.0
0.9
RATIO
1640
1660
1680
1700
1720
1740
1760
1780
1800
WAVELENGTH (A)

Fig. 5

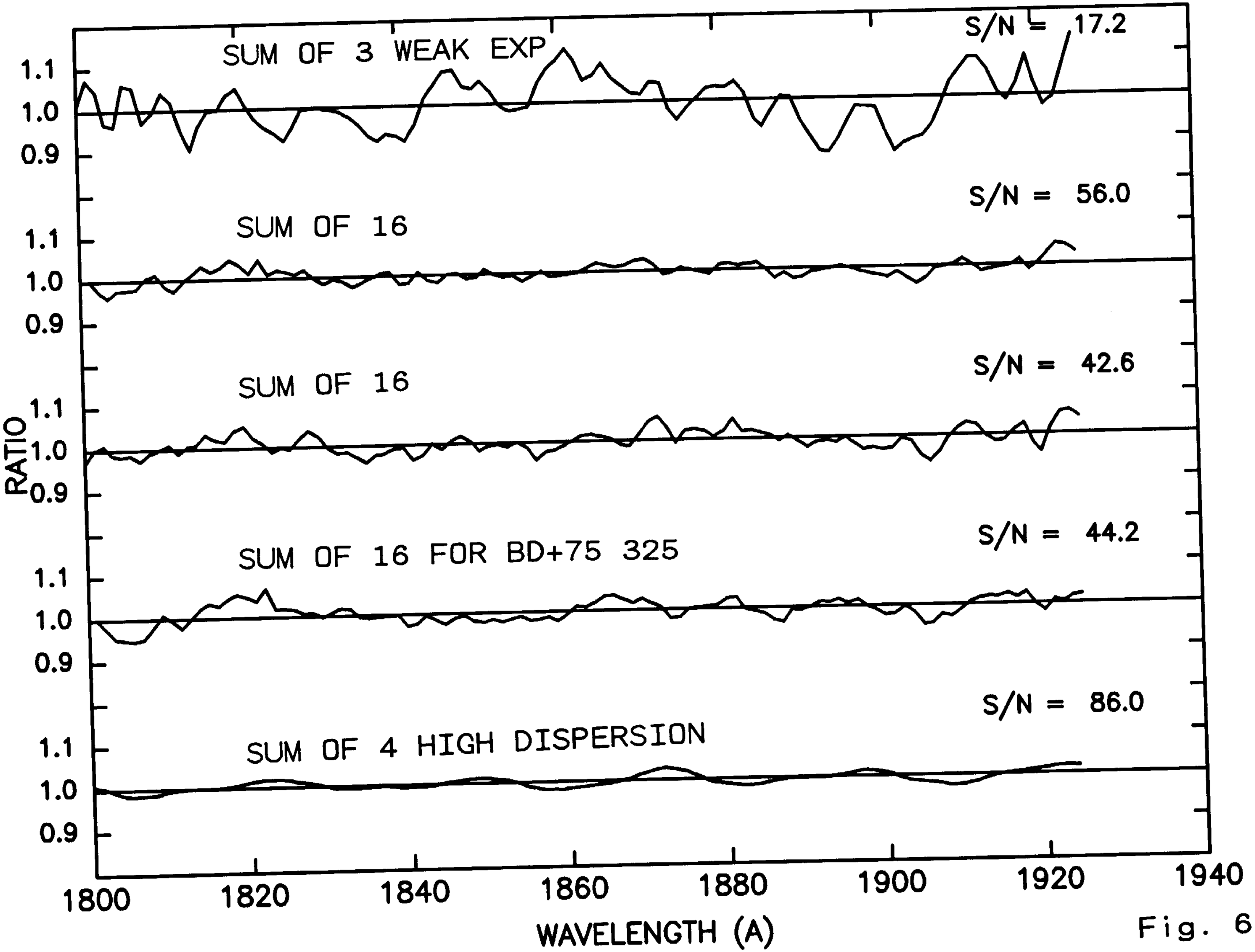
SUM OF 3 WEAK EXP
S/N = 17.2
SUM OF 16
S/N = 56.0
SUM OF 16
S/N = 42.6
SUM OF 16 FOR BD+75 325
S/N = 44.2
SUM OF 4 HIGH DISPERSION
S/N = 86.0
1.1
1.0
0.9
RATIO
1800
1820
1840
1860
1880
1900
1920
1940
WAVELENGTH (A)

Fig. 6

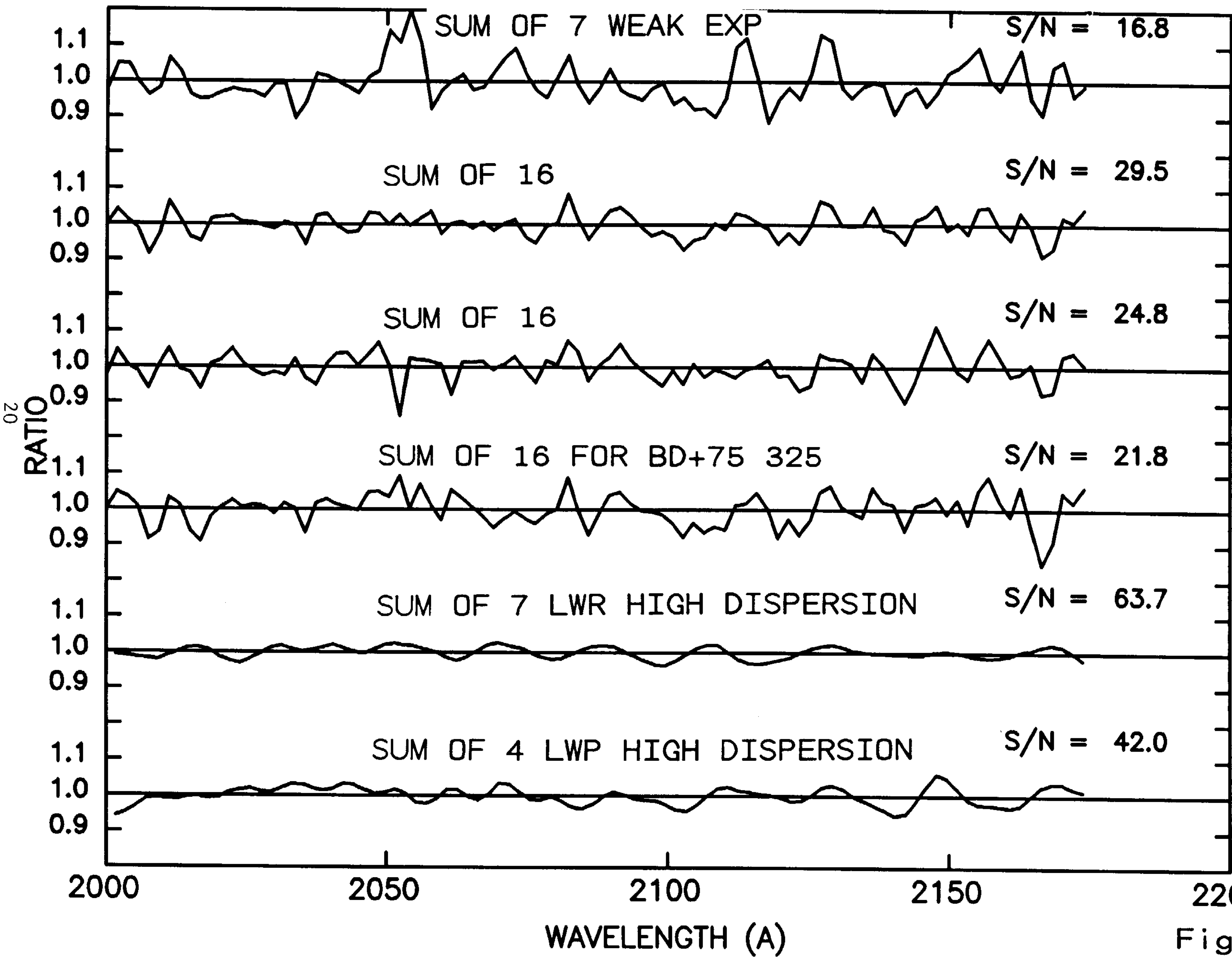
SUM OF 7 WEAK EXP
S/N = 16.8
SUM OF 16
S/N = 29.5
SUM OF 16
S/N = 24.8
SUM OF 16 FOR BD+75 325
S/N = 21.8
SUM OF 7 LWR HIGH DISPERSION
S/N = 63.7
SUM OF 4 LWP HIGH DISPERSION
S/N = 42.0
1.1
1.0
0.9
RATIO
2000
2050
2100
2150
2200
WAVELENGTH (A)

Fig. 7

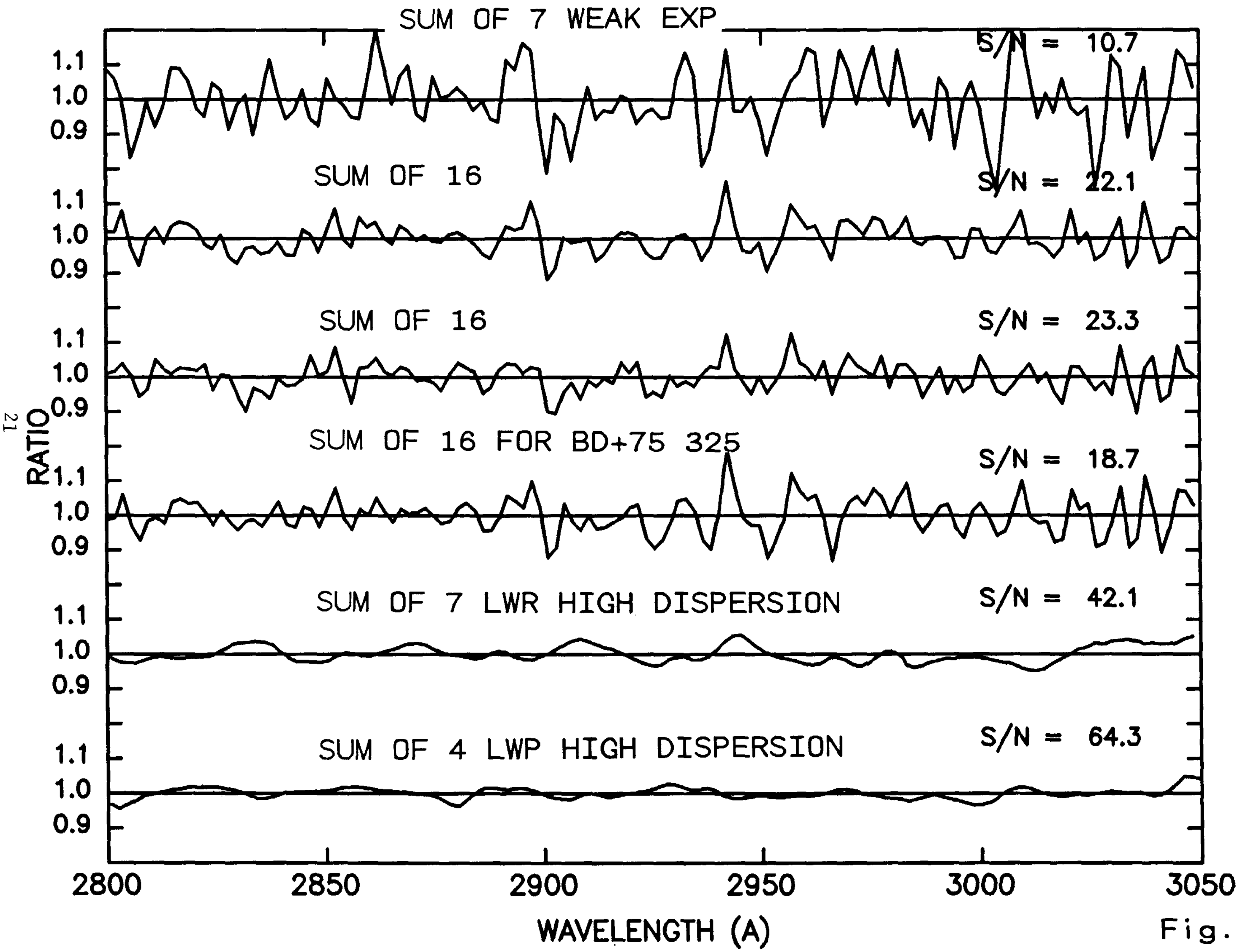
SUM OF 7 WEAK EXP
S/N = 10.7
SUM OF 16
S/N = 22.1
SUM OF 16
S/N = 23.3
SUM OF 16 FOR BD+75 325
S/N = 18.7
SUM OF 7 LWR HIGH DISPERSION
S/N = 42.1
SUM OF 4 LWP HIGH DISPERSION
S/N = 64.3
1.1
1.0
0.9
RATIO
2800
2850
2900
2950
3000
3050
WAVELENGTH (A)

Fig. 8

21

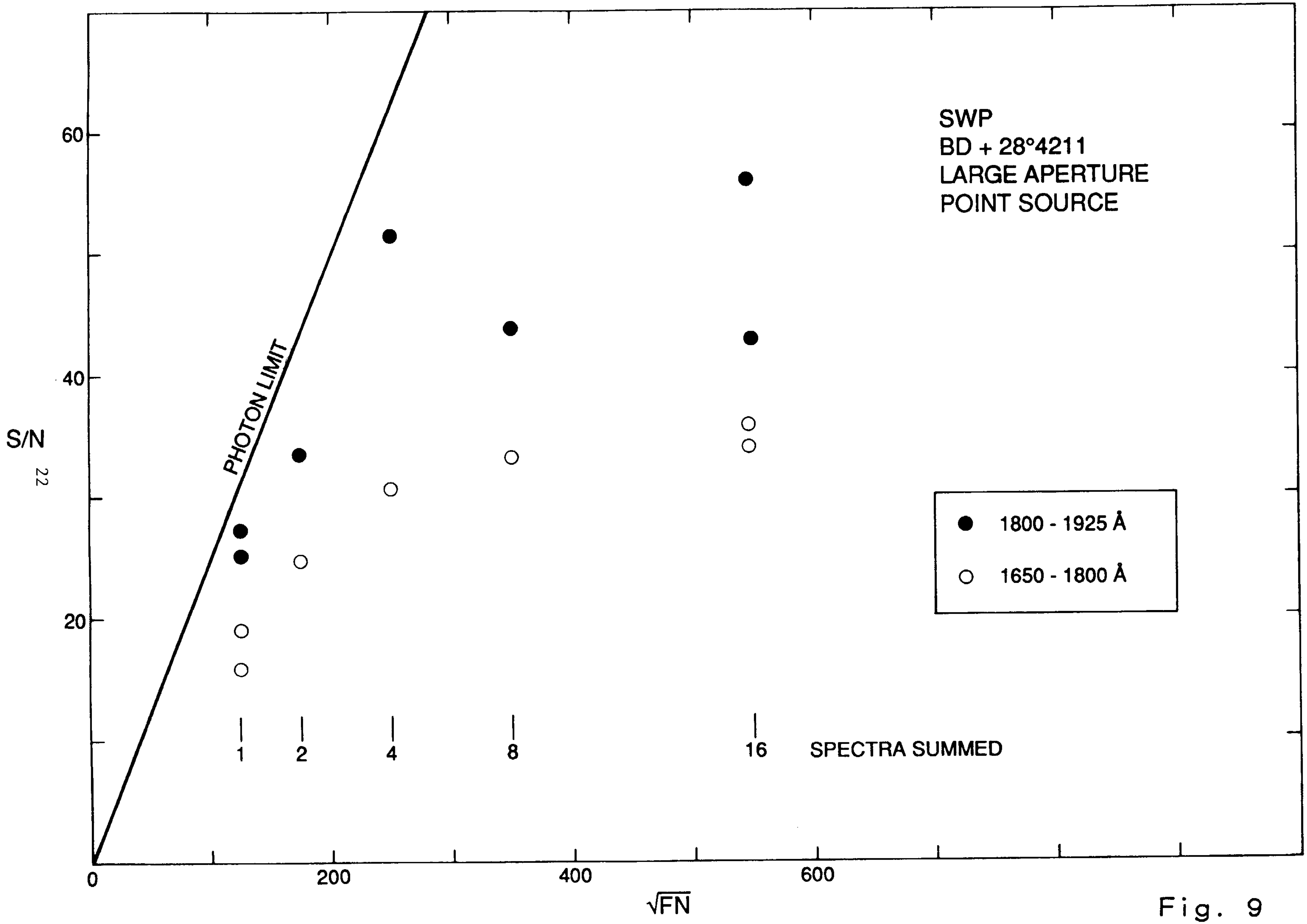
SWP
BD + 28°4211
LARGE APERTURE
POINT SOURCE
PHOTON LIMIT
1800 - 1925 Å
1650 - 1800 Å
1
2
4
8
16
SPECTRA SUMMED
S/N
60
40
20
0
200
400
600
√FN

Fig. 9

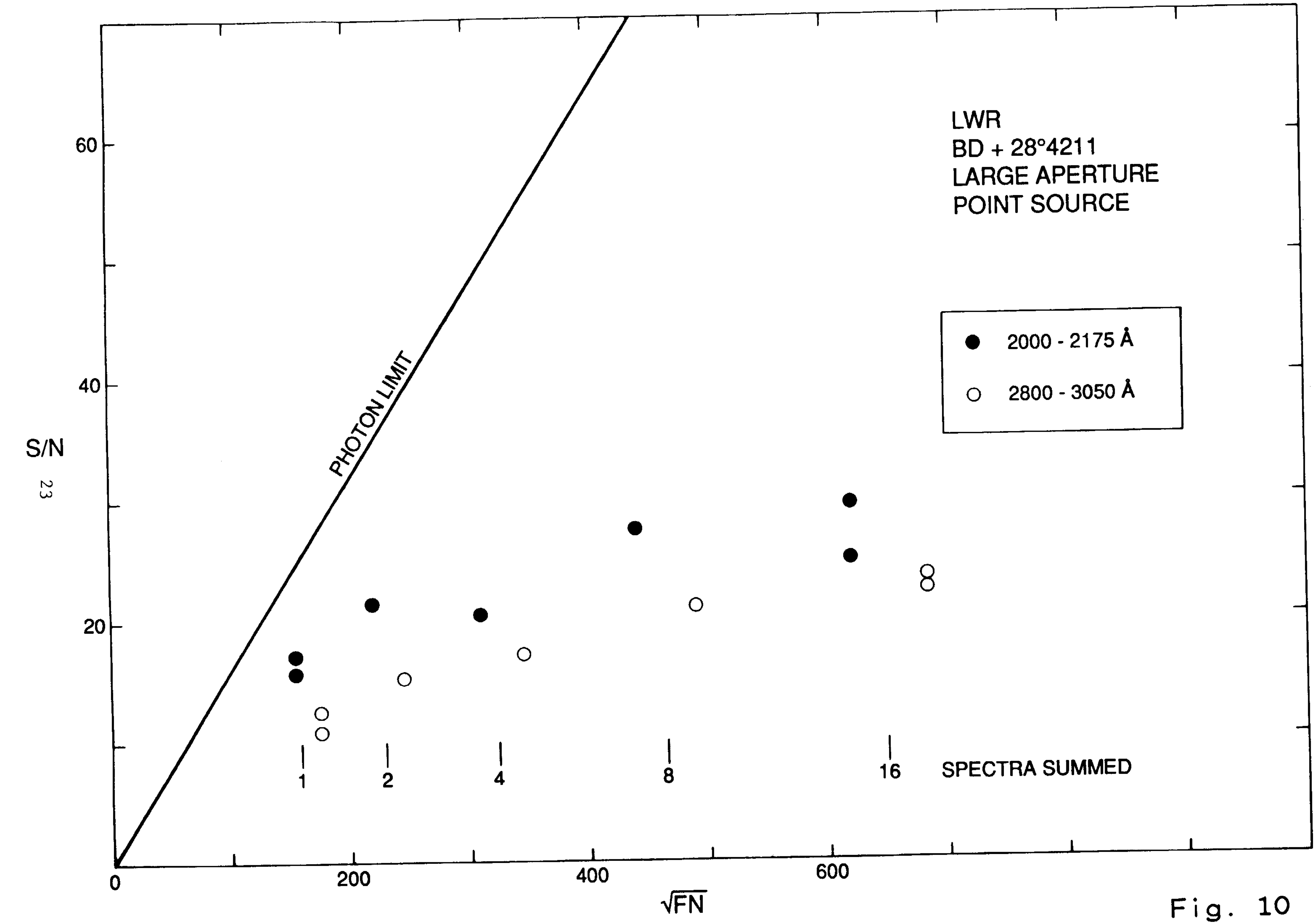

LWR
BD + 28°4211
LARGE APERTURE
POINT SOURCE
2000 - 2175 Å
2800 - 3050 Å
PHOTON LIMIT
S/N
60
40
20
0
200
400
600
√FN
1
2
4
8
16
SPECTRA SUMMED

Fig. 10

23